Supplementary Materials for

Hyperdiverse archaea near life limits at the polyextreme geothermal Dallol area

Jodie Belilla, David Moreira, Ludwig Jardillier, Guillaume Reboul, Karim Benzerara, José M. López-García, Paola Bertolino, Ana I. López-Archilla & Purificación López-García*.

Correspondence to: puri.lopez@u-psud.fr

This PDF file includes:

Figs. S1 to S6
Tables S1 to S5

Other Supplementary Materials for this manuscript include the following:

Data S1 to S7

Data S1. (Table) Organic and ionic chromatography analysis of samples from the Dallol dome and surrounding area.
Data S2. (Table) Identification, phylogenetic affinity and relative abundance of prokaryotic OTUs.
Data S3. Identification, phylogenetic affinity and relative abundance of eukaryotic OTUs from Dallol area samples.
Data S4. Full tree of archaeal 16S rRNA gene fragments in Newick format.
Data S5. Full tree of bacterial 16S rRNA gene fragments in Newick format.
Data S6. Chemical maps obtained from energy dispersive X-ray spectrometry (EDXS) combined to SEM observations of cells and abiotic biomorphs observed in the Dallol area and Lake Assale (Karum).
Data S7. Energy dispersive X-ray spectrometry (EDXS) spectra of different structures observed in samples from the Dallol area.

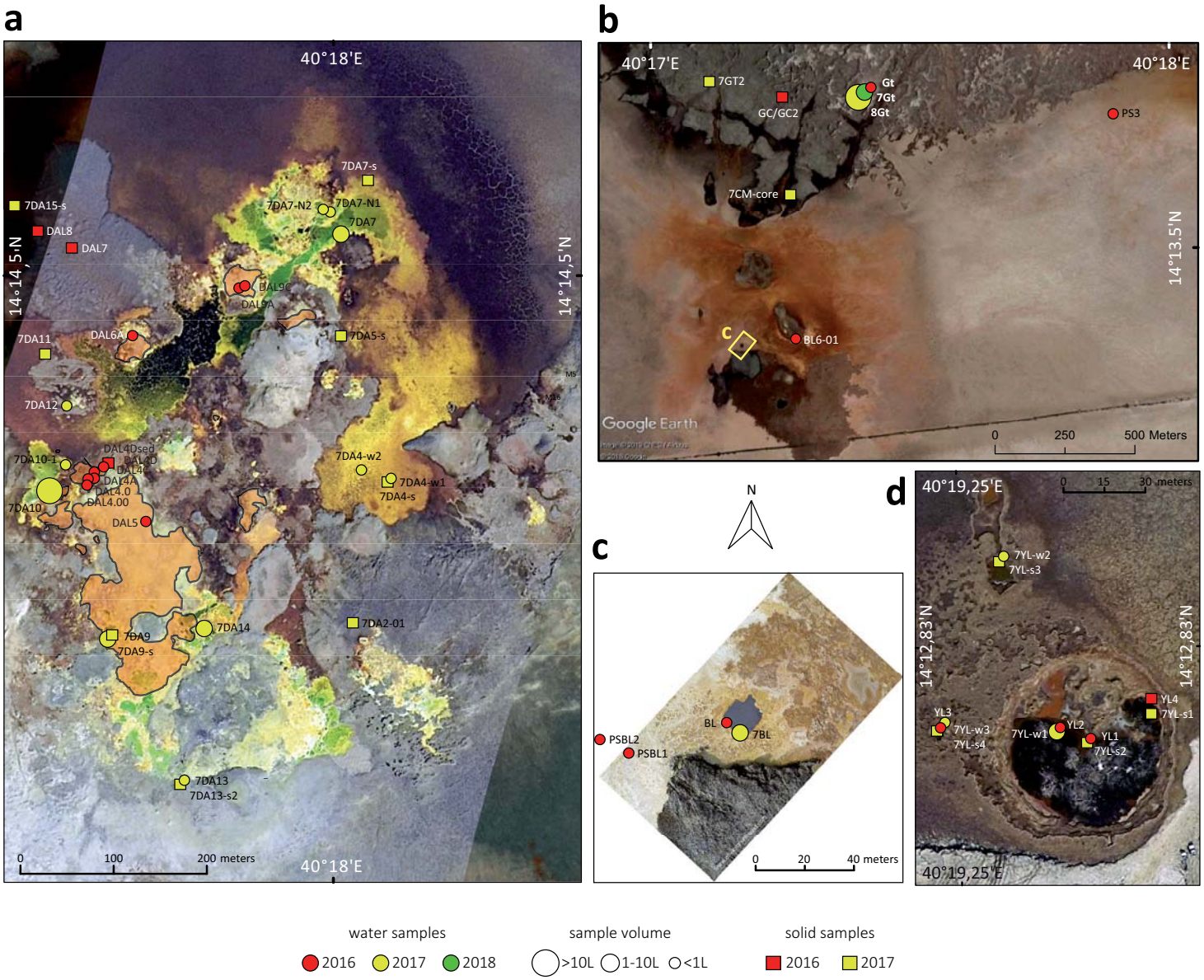

Fig. S1. Aerial view of the main sampling sites in the Dallol area. a, Dallol dome summit showing the acidic green-yellow-brown colored hydrothermal ponds and active degassing areas during our 2017 sampling trip; the orange-shaded area shows the active hydrothermal zone in January 2016. **b**, Dallol West salt canyons and Black Mountain area. **c**, Black Lake. **d**, Yellow Lake and surroundings. Names of samples and sampling sites are indicated. The size of circles is proportional to the water volume collected or filtered for subsequent analyses. Aerial photographs were taken from a drone by O. Grunewald, except b, which is a Google Earth aerial image (09/03/2016) provided by Image © 2019 CNES/Airbus.

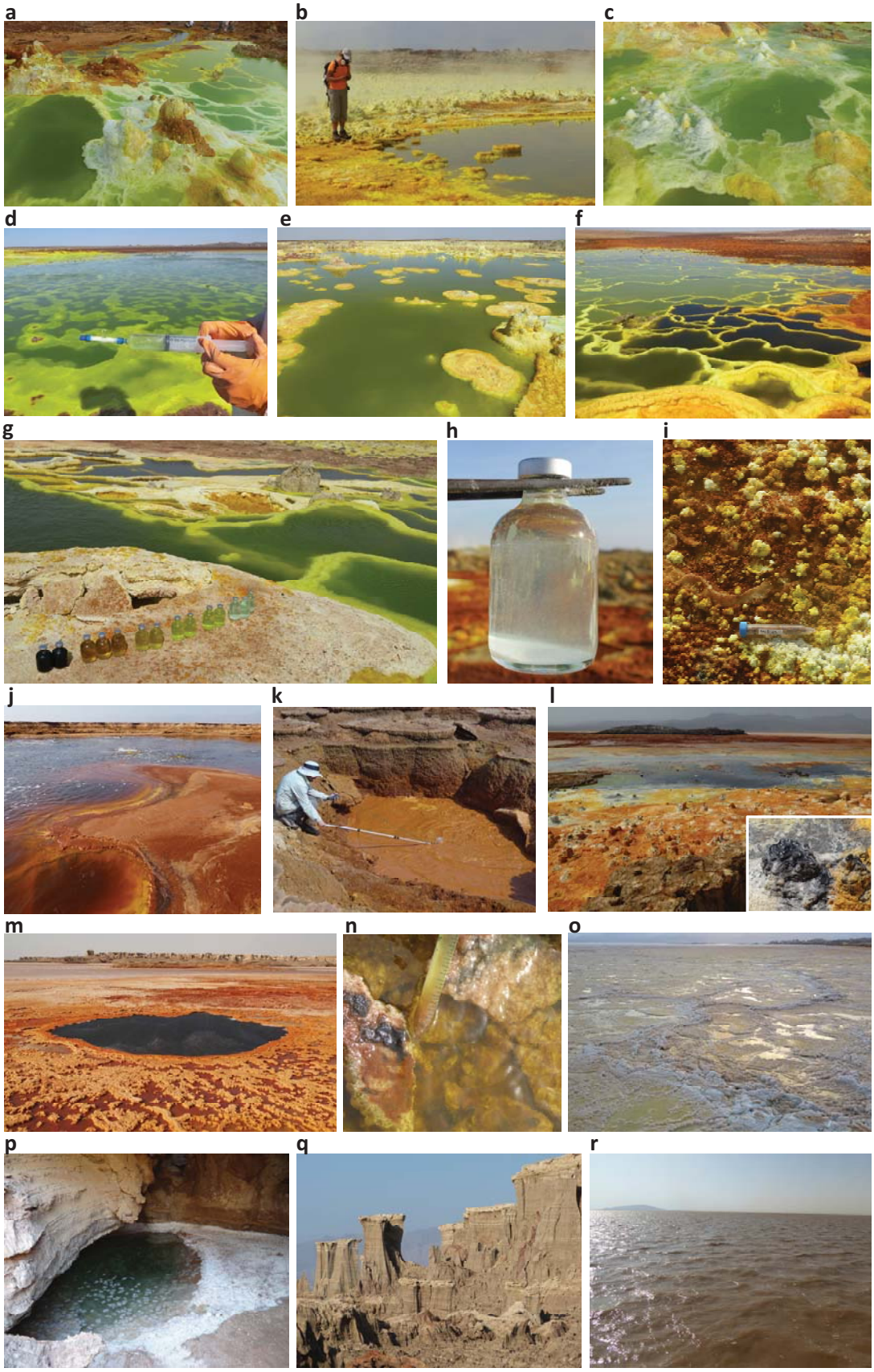

Fig. S2. Views of different sampling sites in the Dallol dome and surroundings in the Danakil Depression. a, DAL4 sampling site ponds; **b**, DAL5 pond and active degassing area; **c**, active hydrothermal springs in DAL9 ponds; **d**, in situ cell-trap filtration at the 7DA7 sampling area; **e**, 7DA9 sampling site; **f**,7DA10 ponds showing increasingly darker and brownish colors along the oxidation gradient; **g**, water samples from the different 7DA10 ponds; **h**, immediate precipitation of halite crystals as water collected from a hot spring (108°C) cools down upon collection; **i**, DAL8 mineral precipitates; **j**, Yellow Lake showing active degassing; **k**, YL3, salt-mud volcano in the Yellow Lake area; **l**, 'Little Dallol' hydrothermal very active area in 2016 on the way to the Black Mountain (in the distance; inlet, chimney emitting hydrocarbon-rich fluids at 110°C); **m**, Black Lake; **n**, PSBL2 (Black Lake area ponds); **o**, wet salt plain, influenced by hydrothermal activity, corresponding to PS3 sample area; **p**, the cave in the salt canyons where Gt, 7Gt and 8Gt samples were collected; **q**, salt canyons; **r**, Assale (Karum) lake. Sample names starting by 7 indicate collection in 2017. Pictures from all other samples/sampling sites were taken during the 2016 expedition.

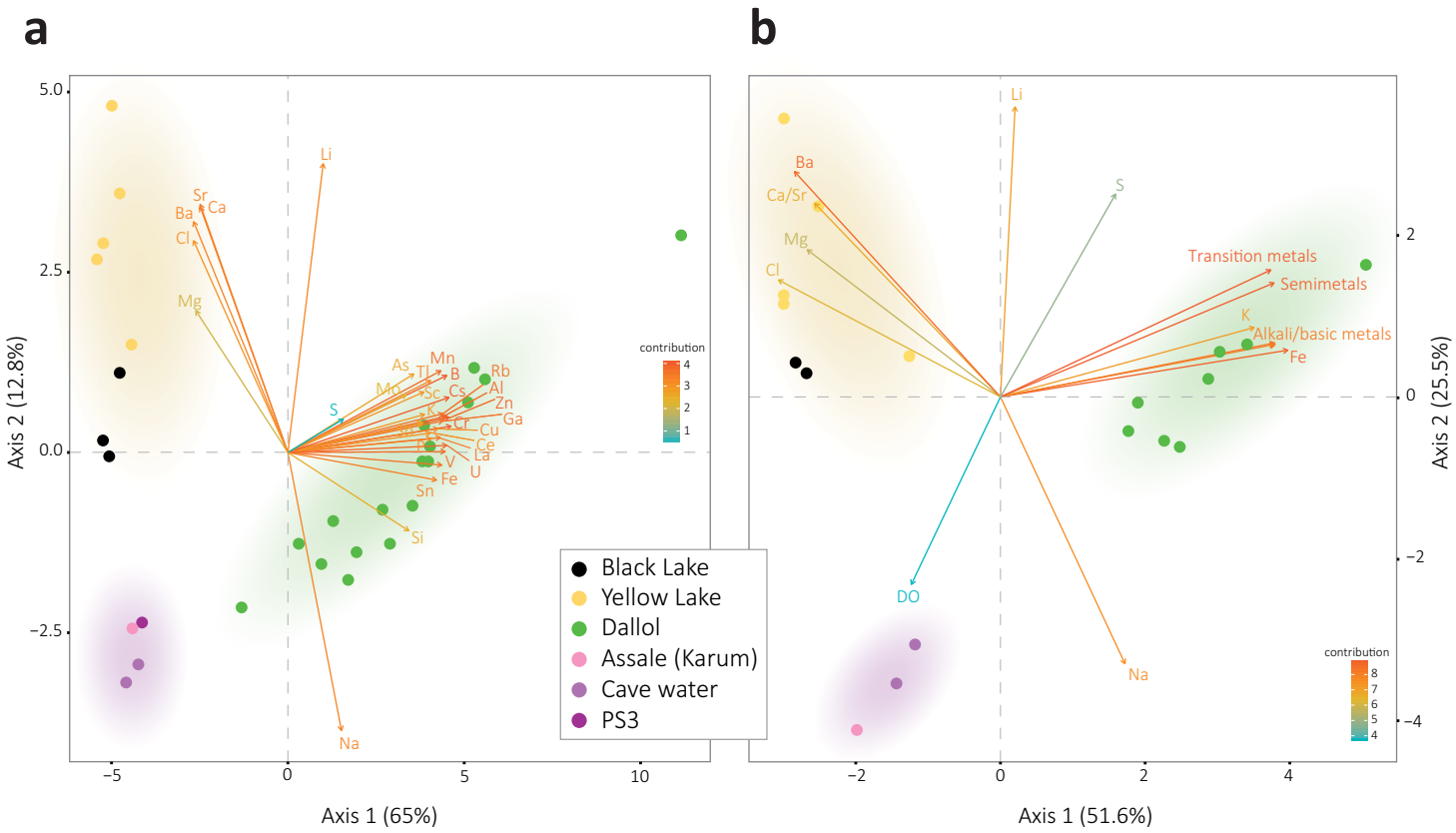

Fig. S3. Principal Component Analyses (PCA) of Dallol area sampling sites as a function of physicochemical parameters. PCA of 29 samples according to their chemical composition; only relatively abundant elements (see Extended Data Table 2) are included in the analysis. A summary of this analysis is shown in Fig.2a. **b**, PCA including the same variables as Fig. 2a but additionally including dissolved oxygen (DO). Measured parameters on site can be found in Extended Data Table 1.

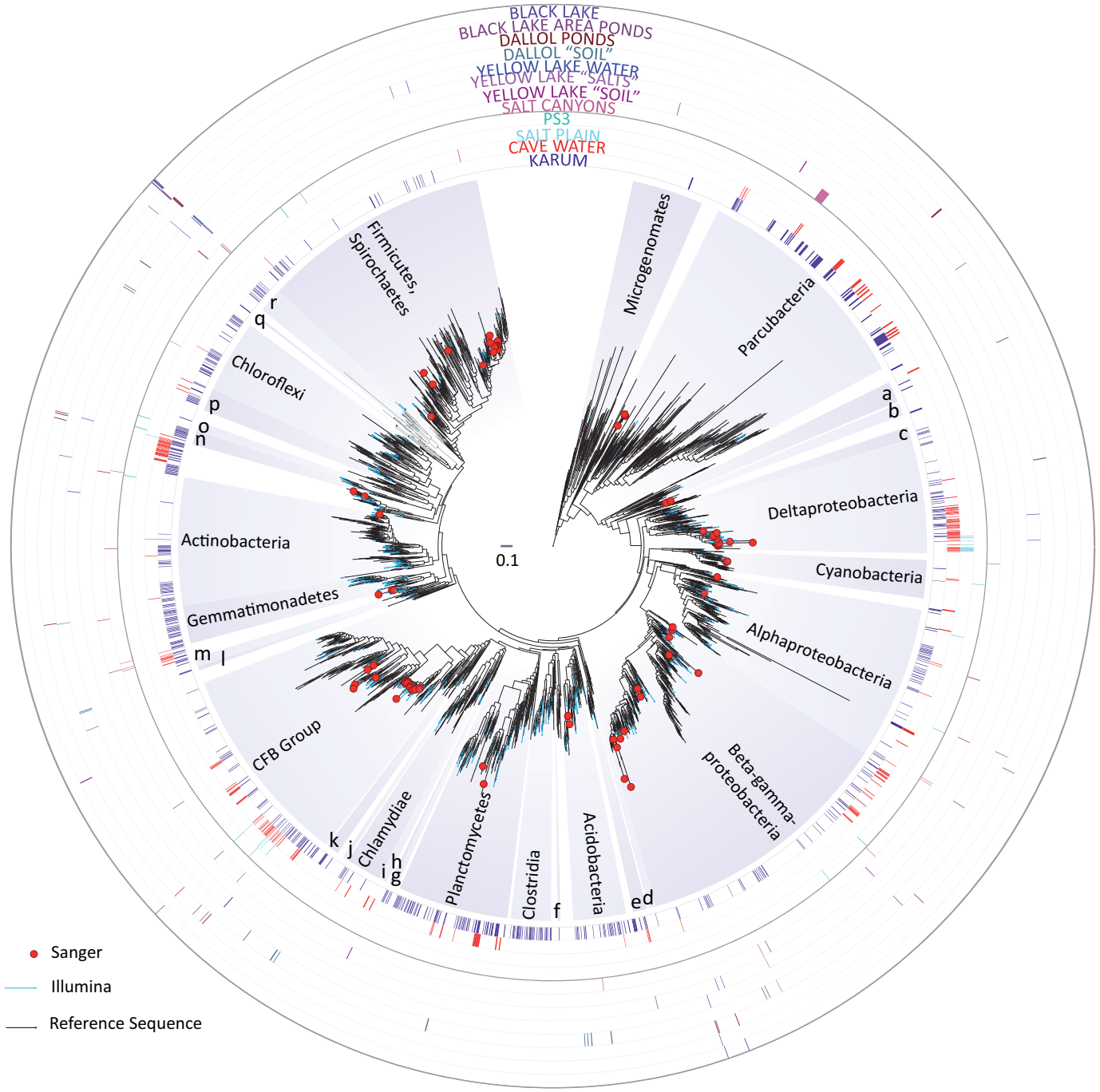

a. Peregrinibacteria
b. Saccharibacteria
c. Desulfovibrionales
d. Deferribacteres
e. Candidate division TM6
f. Candidate division NC10
g. Candidatus Latescibacteria
h. Candidatus BRC1
i. Omnitrophica
j. Zixibacteria
k. Marinimicrobia
l. Rokubacteria
m. Nitrospirae
n. Acetothermia
o. Synergistetes
p. Armatimonadetes
q. Dadabacteria
r. Deinococcus-Thermus

Fig. S4. Phylogenetic tree of bacterial 16S rRNA gene sequences showing the phylogenetic placement of OTUs identified in the different Dallol area samples. Sequences derived from metabarcoding studies are represented by blue lines (Illumina sequences); those derived from cloning and Sanger sequencing of environmental samples, cultures and FACS-sorted cells are labelled with a red dot. Reference sequences are in black. Concentric circles around the tree indicate the presence/absence of the corresponding OTUs in different groups of samples (groups shown in Fig.3a). Only sequences not deemed contaminant (see Supplementary Data S2) were included in the tree. The full tree is provided as Supplementary Data S5.

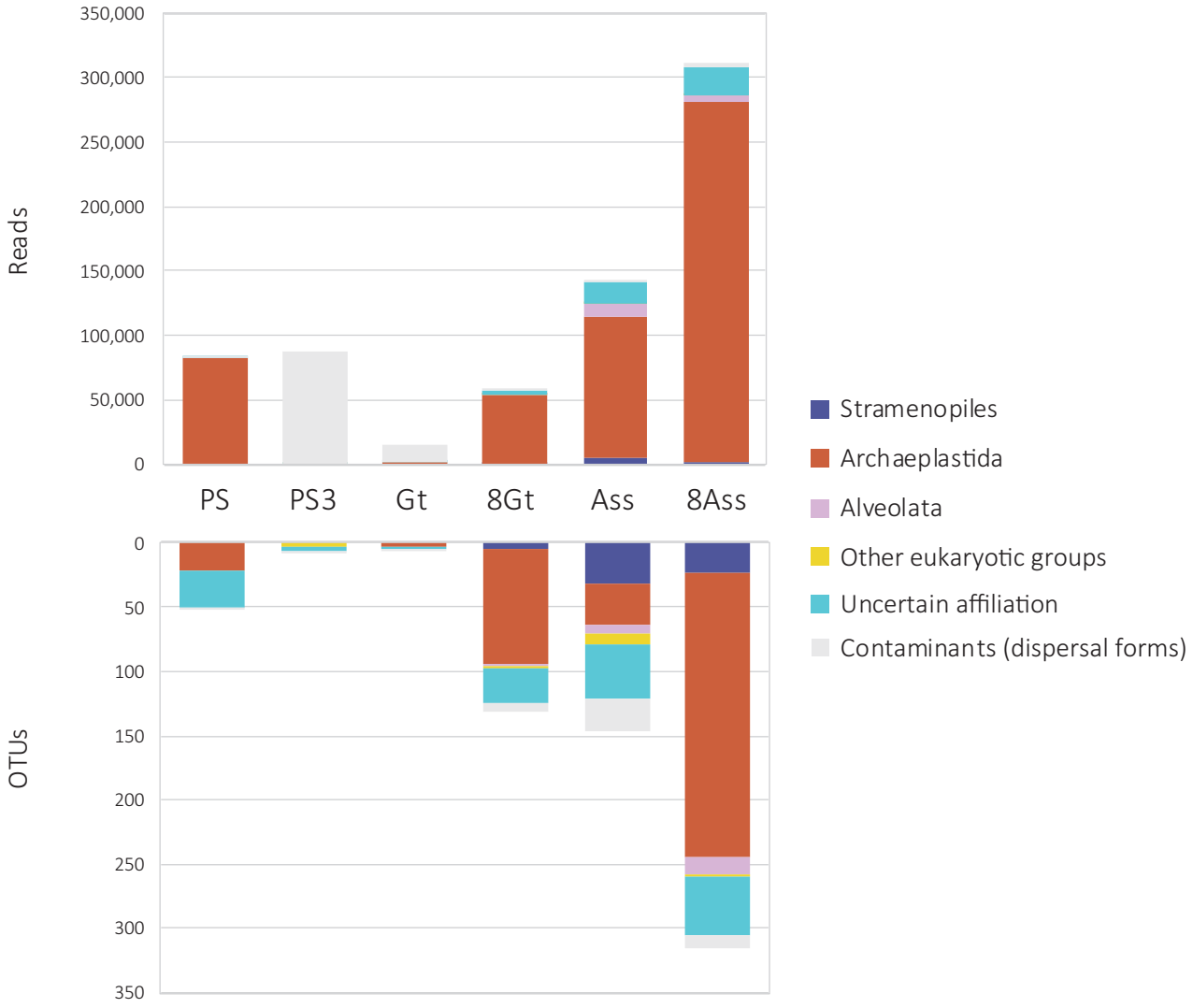

Fig. S5. Eukaryotic presence, diversity and relative abundance in Dallol area samples. Histogram showing the phylogenetic affiliation and abundance of 18S rRNA gene amplicon reads of eukaryotes (upper panel) obtained with universal eukaryotic primers and the associated OTU diversity (lower panel). Only a few samples yielded amplicons; negative PCR controls were always negative. Sequences corresponding to macroscopic plants and fungi (probably derived from pollen or spores) were considered contaminant (light grey). The phylogenetic affiliation of dominant eukaryotic groups is color-coded.

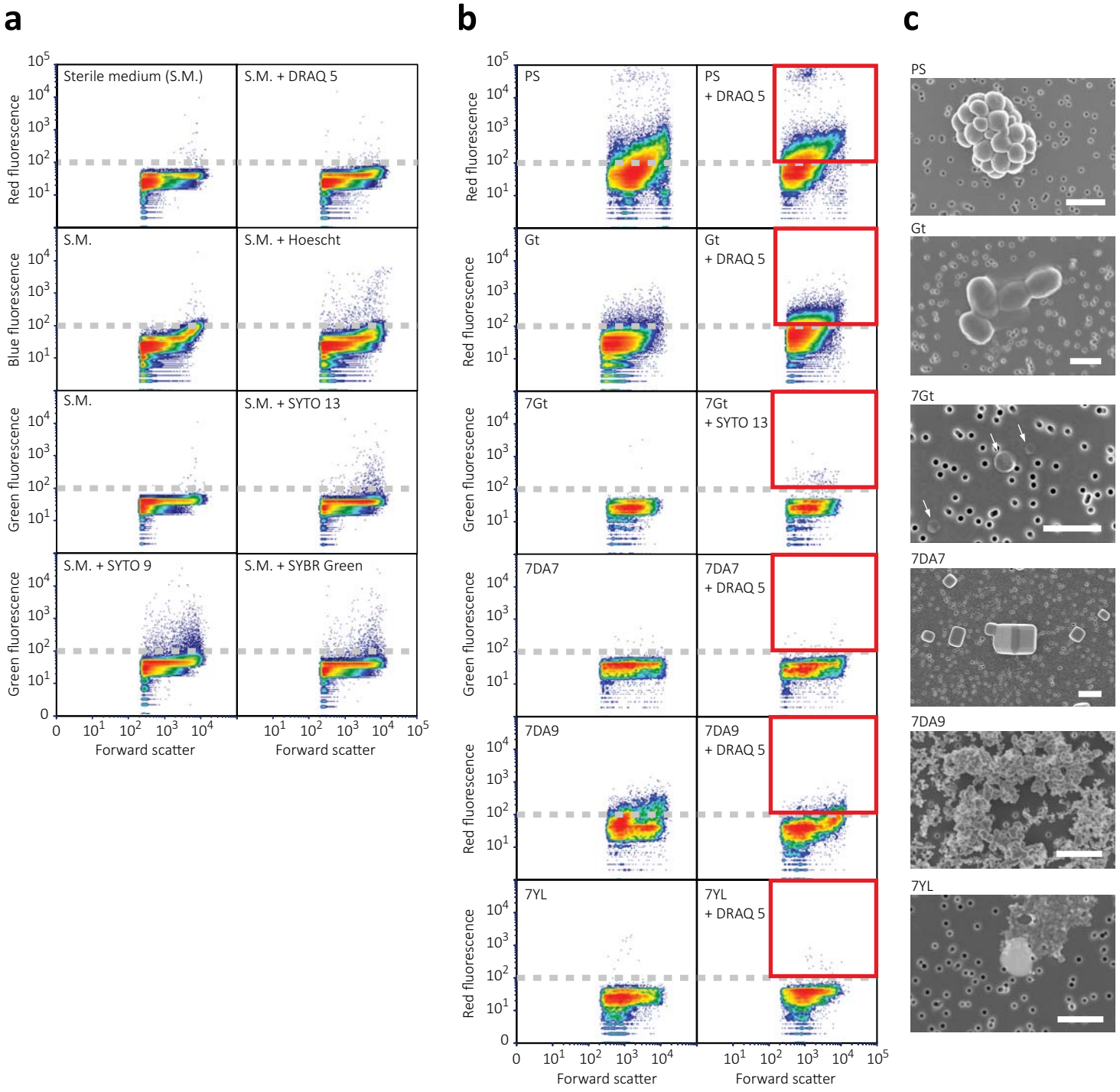

Fig. S6. Multiparametric fluorescence analyses and fluorescence-activated cell sorting (FACS) analyses of representative Dallol area samples. a, effect of DNA fluorescent dyes on background fluorescence emission; natural (left panels) and DNA dye-induced (right panels) fluorescence in the sterile hypersaline SALT-YE medium used to dilute/sort Dallol samples. Fluorescence is plotted against the size of the analyzed particles (forward scatter); events concentration is color-coded, red being high concentration and blue, low concentration. DRAQ 5 and SYTO 13 introduced less background and were chosen for FACS of natural samples. The approximate background threshold (ca. 102) is indicated by a broken grey line. **b**, multiparametric fluorescence analyses of different Dallol samples before (left panels) and after (right panels) adding fluorescent DNA dyes. Events (particles) above background (red squares) were FACS-sorted and filtered on 0.1 µm pore-size filters prior to SEM observations. **c**, SEM photographs showing examples of sorted particles. Cells are observed in samples PS, Gt and 7Gt; halite crystals in 7DA7 and amorphous mineral particles in 7DA9 and 7YL. Arrows indicate ultrasmall cells. The scale bar is 1 µm.

Table S1. List and description of samples from the Dallol area analyzed in this study and type of analyses performed. DO, dissolved oxygen; ORP, oxido-reduction potential; a_w, water activity. SEM/XRD, scanning electron microscopy/x-ray diffraction analyses; FACS, fluorescence-activated cell sorting analysis; n.a., not applicable; n.d. not determined.

Color of ponds or solid samples	Sample name	Coordinates	Collection date	Brief description	Sample type / volume			Physicochemical parameters							Type of analyses					
					Solid	Liquid (ml)	0.2-30 µm fraction (ml)[a]	Temp (°C)	pH	DO (%)	DO (mg/l)	ORP (mV)	Salinity (%)[b]	a_w	Chemistry	Cloning/ Sanger seq.	Meta-barcoding	Culture assays[c]	SEM/ XRD	FACS
Dallol hydrothermal ponds																				
	DAL4.00	14.23916N 40.297059E	16.01.2016	Hydrothermal fluid from a salt chimney feeding cascading ponds along redox gradient site DAL4		50	1000	108,0	n.d	n.d	n.d	n.d	30,0	0,719	X	X				
	DAL4.0	14.23923N 040.29707E	17.01.2016	Warm whitish green pond in the redox pond series DAL4		50	1000	46,3	-0,43	0,55	0,03	328,95	21,0	n.d	X	X	X	Y	X	
	DAL4A	14.23921N 040.29713E	17.01.2016	Bright green pond in the redox pond series DAL4		50	1000	30,5	-0,53	3,05	0,26	366,8	22,0	n.d	X	X	X	Y	X	
	DAL4C	14.23967N 040.29744E	16.01.2016	Brownish green pond in the redox pond series DAL4			1000	31,6	-0,95	1	0,08	384,05	21,5	n.d		X	X	Y		
	DAL4D	14.23934N 040.29728E	16.01.2016	Dark brown pond along an oxidation gradient, DAL4 site		50	1000	31,0	-0,72	1,4	0,11	381,55	n.d	n.d	X	X	X	Y	X	
	DAL 4D-SED	14.23934N 040.29728E	16.01.2016	Yellow salt front forming pond wall	X			n.a	n.a	n.a	n.a	n.a	n.a	n.d	X	X				
	DAL 5	14.23869N 40.29776E	17.01.2016	Yellow water from one big Dallol pond		50		42,6	-0,93	3,4	0,19	373,3	40	n.d				Y		
	DAL6A	14.24083N 040.29756E	18.01.2016	Fluid from a salt chimney feeding various ponds along an oxidation gradient, site DAL6		50	1000	108,4	-0,65	n.d	n.d	n.d	n.d	n.d	X	X	X	Y		
	DAL 7	14.242343N 40.296798E	18.01.2016	Sulfur-colored mineral precipitates on "chocolate formation"	X			n.a	n.a	n.a	n.a	n.a	n.a	n.d				Y		
	DAL8-01	14.24217N 040.29635E	20.01.2016	Yellow, potentially sulfur-rich precipitates	X			n.a	n.a	n.a	n.a	n.a	n.a	n.d		X	X	Y		
	DAL8-02	14.24217N 040.29635E	20.01.2016	Golden, potentially sulfur-rich salt precipitates	X			n.a	n.a	n.a	n.a	n.a	n.a	n.d		X	X			
	DAL8-03	14.24217N 040.29635E	20.01.2016	Brown, potentially sulfur-rich salt precipitates	X			n.a	n.a	n.a	n.a	n.a	n.a	n.d		X	X			
	DAL9A	14.241504N 40.298836E	21.01.2016	Large ligth green bubbling pond with various hydrothermal sources; site DAL9		50	650	37,9	-0,27	n.d	n.d	n.d	n.d	n.d	X	X	X	Y		
	DAL9C	14.24151N 40.298874E	21.01.2016	Smaller deep green hydrothermal pond at the DAL9 site		50	750	56,0	-0,20	n.d	n.d	n.d	n.d	n.d	X	X	X			
	7DA2-01	14.241275N 40.300633E	06.01.2017	Grey cauliflower-like mineral precipitates	X			n.a	n.a	n.a	n.a	n.a	n.a	n.d		X	X			
	7DA4-w1	14,239406N 40,300419E	10.01.2017	Yellow-brownish water from a drying pond formed by yellow-colored salt		100		27,9	-0,73	3,8	0,13	416,1	44	0,667	X					
	7DA4-w2	14,239892N 40,300106E	10.01.2017	Slightly lighter water from the same kind of pool as 7DA4-w1		100		27,0	-0,72	2,9	0,09	420,1	40	0,698	X					
	7DA4-s	14,239406N 40,300419E	10.01.2017	Fresh, yellow cauliflower-like mineral precipitates near 7DA4-w2	X			n.a	n.a	n.a	n.a	n.a	n.a	n.d		X	X			
	7DA5-s	14,240908N 40,300119E	10.01.2017	Brown (oxidized), fluid-impregnated cauliflower-like mineral precipitates	X			n.a	n.a	n.a	n.a	n.a	n.a	n.d	X	X	X			
	7DA7	14.24219N 40.300102E	07.01.2017	Water from an active green large pond fed by multiple hydrothermal springs		500	3000	19,7	-0,55	4,1	0,16	371,9	47	0,694		X	X	X	X	X
	7DA7-s	14.2428N 40.300494E	10.01.2017	Brown salt crust East to 7DA7 active site on a drying pondcovering a layer of wet yellow salt	X			n.a	n.a	n.a	n.a	n.a	n.a	n.d	X					
	7DA7N-1	14.242381N 40.299992E	10.01.2017	Bluish hot pond on the northern terrace feeding 7DA7		50		44,6	-0,33	5,7	0,16	271,2	40,0	0,694	X			Y		
	7DA7N-2	14.242381N 40.299992E	10.01.2017	Hotter, greenish pond adjacent to 7DA7N-1		50		68,0	n.d	n.d	n.d	n.d	37,0	0,698	X					
	7DA9	14.241528N 40.29884E	08.01.2017	Large pond in active degassing area with many white-yellowish chimneys and salt nenuphars		500	6000	31,9	-0,34	5,5	0,16	369	43	0,708	X	X	X	X	X	X
	7DA9-s	14.241528N 40.29884E	08.01.2017	Centimetric round-shaped salt and sulfur formations in a dry pond next to 7DA9	X			n.a	n.a	n.a	n.a	n.a	n.a			X	X			
	7DA10	14.23908N 40.296598E	09.01.2017	Upper green pond in a well-marked terrace system along an oxidation gradient		100	14700	55,2	-0,08	2,2	0,05	321,8	35,0	0,714	X	X	X			
	7DA10-1	14.23908N 40.296598E	09.01.2017	Highly evaporated, dark brown pond, lower in the 7DA10 terrace system		100		33,4	n.d	n.d	n.d	n.d	70	0,580	X			Y		
	7DA12	14.240136N 40.29675E	10.01.2017	Active chimney (nearby 2016 site DAL6)		100		108,3	0,47	n.d	n.d	n.d	43,0	n.d	X					
	7DA13-w1	14.235495N 40.298135E	11.01.2017	Hydrothermal fluid from big grey active chimney		100		103,6	n.d	n.d	n.d	n.d	35,0	0,723	X					
	7DA13-s2	14.235495N 40.298135E	11.01.2017	Grey, hard salt fragments at the bottom of chimney 7DA13	X			n.a	n.a	n.a	n.a	n.a	n.a	n.d		X	X			
	7DA14	14.237398N 40.298428E	12.01.2017	Central pond in active group of geothermal ponds. Green color		50	675	39,7	-0,51	2,4	0,15	382	40	0,748	X	X	X			
	7DA15-s	14.2421427N 40.297727E	13.01.2017	Green/yellow sediment near the "chocolate formation" CH-F	X			n.a	n.a	n.a	n.a	n.a	n.a	n.d		X	X			
Yellow Lake (Gaet'Ale)																				
	YL1	14.213574N 40.32128E	19.01.2016	Yellow Lake bubbling water, yellow-orange color, oily textyre, smell of organics-containing gas	X	50	400	40,6	1,88	6,6	0,37	447,1	>50	n.d	X	X	X	Y	X	
	YL2	14.213648N 40.321188E	19.01.2016	Yellow Lake bubbling water - nearby spot (few meters away)		50	400	39,5	1,88	5,4	0,35	419,3	51,0		X	X	X	Y		
	YL3-01-w	14.213598N 40.320748E	19.01.2016	Water from salt/sediment volcano			400	37,1	n.d	n.d	n.d	n.d	>50	0,319		X	X	Y	X	
	YL3-01-s	14.213598N 40.320748E	19.01.2016	Salty deposits from bubbling salt/sediment volcano - reddish color	X			37,1	n.a	n.a	n.a	n.a	n.a	n.d		X	X			
	YL4-01	14.21386N 40.321482E	19.01.2016	Salt crust on top of sediment at the further upper rim of Yellow Lake	X			n.a	n.a	n.a	n.a	n.a	n.a	n.d		X	X			
	7YL-w1	14.213574N 40.32128E	12.01.2017	Water from the Yellow Lake		150	5000	37,4	1,52	11,5	0,63	462,2	>50	0,261	X			X	X	
	7YL-w2	14.213648N 40.321188E	12.01.2017	Water from a mid-sized pond near the Yellow Lake, strong smell of organics, dead birds		200		33,8	2,40	4,4	0,20	310,3	70	0,467	X			X		X
	7YL-w3	14.213598N 40.320748E	12.01.2017	Water from salt mud volcano (YL3 in 2016)		100		35,9	1,37	5,1	0,32	349,3	80		X			X		
	7YL-s1	14.213574N 40.32128E	12.01.2017	Salt crust from dried area in Yellow Lake	X			n.a	n.a	n.a	n.a	n.a	n.a	n.d		X	X			
	7YL-s2	14.213648N 40.321188E	12.01.2017	Pinkish salt forming ripple marks on the rim of the Yellow Lake	X			n.a	n.a	n.a	n.a	n.a	n.a	n.d		X	X			
	7YL-s3	14.213598N 40.320748E	12.01.2017	Salt fragments from rim of 7YL-w2	X			n.a	n.a	n.a	n.a	n.a	n.a	n.d	X	X	X			
	7YL-s4	14.2136083N 40.3212611E	12.01.2017	Reddish salt/sediment from salt mud volcano	X			n.a	n.a	n.a	n.a	n.a	n.a	n.d		X	X			
Black Lake and surroundings																				
	PSBL1	14.221732N 40.28582E	19.01.2016	Reddish salt and water from pond close to Black Lake		50		40,6	2,63	n.a	n.a	n.a	62,0	0,334		X	X	XY		
	PSBL2	14.221788N 40.285713E	19.01.2016	Yellowish salt and water from pond close to Black Lake		50		40,6	2,50	n.a	n.a	n.a	58,0	0,345		X	X	XY		
	PSBL3	14.22173N 040.28582E	19.01.2016	Orange salt and water from pond between Black Lake and camp site		50		n.d	n.d.	n.a	n.a	n.a	34,0	0,722				XY	X	
	PSBL4	14.22173N 040.28582E	22.01.2016	Warm red pond with acid emissions		50		40,0	3,50	n.a	n.a	n.a	38,0	0,711				X	X	
	BL2	14.221842N 40.286173 E	19.01.2016	Black Lake bischofite-enriched water, very high viscosity		25		n.a	n.a	n.a	n.a	n.a	n.a	n.d		X				
	BL / BL1-02 / BL-w	14.22182N 40.286208E	19.01.2016	Black Lake bischofite-enriched water, very high viscosity		50	150	70,6	3,50	n.a	n.a	n.a	n.a	0,319	X	X	X	Y		
	BL6-01	14.22211N 40.28805E	24.01.2016	Black fluid from chimney in very active young geothermal formation, black dome area		15		110,0	4,40				n.d	n.d				Y		
	7BL-w1	14.22182N 40.286208E	10.01.2017	Black Lake bischofite-enriched water from surface		150		60,1	2,57	2,8	0,11	226,9	76	0,322	X		X	X		
	7BL-w2	14.22182N 40.286208E	10.01.2017	Black Lake bischofite-enriched water, 3 m depth		100		n.a	n.a	n.a	n.a	n.a	n.a	n.d	X		X	Y		
Salt plain at Dallol dome base																				
	PS	14.2250194N 40.2889000E	19.01.2016	Salt pan fragment between the Dallol dome and Black Lake, rehydrated with sterile spring water	X	100	30	n.a	n.a	n.a	n.a	n.a	n.a	n.d		X	X	X	X	X
	PS3	14.22912N 40.297935E	19.01.2016	Water from salt shallow, hydrothermally influenced, pond at the dome base		150	950	29,3	4,21	n.d	n.d	n.d	20,0		X	X	X	XY	X	
Lake Assale (Lake Karum)																				
	Ass	14.089567N 40.348583E	23.01.2016	Water from Lake Assale (Karum), overflooded towards the North of the Danakil Depression			8000	26,2	6,68	53,0	4,30	97,7	20,0	n.d		X	X	X		
	8Ass	14.089567N 40.348583E	15.01.2018	Water from Lake Assale (Lake Karum)		100	3000	22,0	6,54	14	2,82	221	31	0,718	X	X		XY	X	
Dallol Salt Canyons																				
	Gt	14.229704N 40.289952E	18.01.2016	Cave hypersaline water reservoir at the salt canyons, West Dallol dome		50	50	n.d	n.d	n.d	n.d	n.d	30	0,728		X	X	XY	X	X
	7Gt	14.229704N 40.289952E	11.01.2017	Cave hypersaline water reservoir at the salt canyons, West Dallol dome		100	10000	29,0	6,27	9,5	0,27	117,2	30	0,729		X	X	XY	X	X
	7Gt2	14.23043N 40.285295E	13.01.2017	Small core at the mouth of a dry subterranean stream bed at the Western Dallol salt canyons	X			n.a	n.a	n.a	n.a	n.a	n.a	n.d		X	X			
	8Gt-0.22	14.23043N 40.285295E	16.01.2018	Cave hypersaline water reservoir at the salt canyons, West Dallol dome		100	3000	22,0	6,54	15,2	2,30	262,1	30	0,731	X	X			X	
	GC/GC2	14.229658N 40.287723E	15.01.2016	Gypsum crust from Dallol West salt canyons	X			n.a	n.a	n.a	n.a	n.a	n.a	n.d	X	X	X			
	7CM-core	14.226668N 40.287813E	13.01.2017	Small core of hydrothermally-influenced orange salty mud core at the base od the dome	X			n.a	n.a	n.a	n.a	n.a	n.a	n.d		X	X			

[a] Volume of water filtered to retain particles/cells in the indicated size range
[b] Salinity values taken with a refractometer
[c] Samples labeled X and Y represent independent culture assays in two different laboratories (X-Orsay, Y-Madrid)

Table S2. Chemical composition of samples from the multi-extreme area of Dallol. For details about chemical analyses, see Methods. Data about organic compounds identified in Dallol samples are listed in Supplementary Data S1.

Liquid samples

Element	Concentration (mg/ml)																												
	DAL4.00	**DAL4.0**	**DAL4A**	**DAL4D**	**DAL6A**	**DAL9A**	**DAL9C**	**7DAL4-W1**	**7DAL4-W2**	**7DAL7**	**7DAL7-N1**	**7DAL7-N2**	**7DAL9**	**7DAL10**	**7DAL12**	**7DAL13-W1**	**7DAL14**	**BL**	**7BL-W1**	**7BL-W2**	**YL1**	**YL1-2 (YL2)**	**7YL-W1**	**7YL-W2**	**7YL-W3**	**PS3**	**7Gt**	**8GT**	**8Ass**
Cl	105190	111510	22610	99430	126750	123950	136920	170680	144790	201890	192280	179610	149770	170150	191470	161980	172310	194550	208200	220160	285390	373800	283480	255200	325980	149280	146110	230449	248886
Na	93210,36	105537,04	85029,17	81641,76	107204,75	95246,84	114638,67	39699,19	54954,80	51558,63	56742,29	59563,51	64186,60	69668,23	87876,56	85356,59	61908,40	1764,03	1541,54	1607,32	2616,01	2375,56	1441,97	5149,17	1652,79	93924,71	89081,01	144416,34	112833,19
Ca	2263,99	2867,06	2788,01	3388,86	1055,45	2390,61	3059,76	7937,79	6169,13	4301,43	4767,66	3892,18	6084,12	3774,66	1158,84	6123,51	6707,38	13436,28	8071,31	8306,92	163132,50	192095,04	175942,77	111085,94	162942,51	20316,50	6929,85	4037,16	23148,69
Mg	3764,86	4550,75	4387,41	6127,92	4538,48	6269,98	6268,84	9790,36	6348,22	6440,81	7206,49	5872,36	4249,59	3099,97	3131,56	2123,95	5260,42	145295,05	108652,70	112683,58	53922,80	60599,66	41427,89	37276,85	42199,86	10953,71	1914,20	1778,91	4148,39
Fe	26445,16	33578,06	32990,09	44030,37	32940,60	41621,88	40293,36	46182,85	29064,79	45206,84	47342,72	39815,45	23675,95	23107,07	26107,32	5337,40	24115,73	2719,04	1505,35	1488,73	91,65	74,52	81,98	418,42	324,10	0,00	2,18		0,09
K	9047,00	17096,11	16445,10	22355,01	16684,14	22301,91	21746,24	28073,69	17451,30	23683,71	24945,93	21539,29	13469,45	12000,32	12859,23	4421,73	14975,34	820,22	2323,18	2213,50	6186,46	4735,97	3834,52	24950,94	4617,63	7047,53	4737,88	2729,60	4759,99
S	2027	2077	2529	2984	3479	3111	3070	1836	2306	1240	1180	881	1560	1112	1840	2340	1543	1648	ND	ND	2427	3092	660	410	450	1384	351		
Mn	673,24	853,16	847,55	1141,84	858,47	1121,10	1129,63	1551,99	1023,92	1281,68	1343,48	1169,53	773,03	696,02	691,42	283,56	860,66	393,63	206,67	208,93	381,84	442,58	362,36	251,53	385,35	89,69	1,54	1,61	5,11
Sr	68,06	85,09	84,34	108,12	41,38	72,39	81,61	188,87	124,26	104,78	117,33	98,58	122,28	93,31	40,41	77,33	118,49	331,62	186,03	186,68	3042,29	3462,02	2885,69	2032,27	2747,67	439,81	159,94	98,52	372,42
B	353,15	456,40	457,15	608,86	369,37	470,06	504,49	899,60	591,48	529,14	607,12	486,72	491,64	379,03	297,55	233,89	547,38	146,22	125,20	98,88	190,02	215,02	179,76	148,99	187,95	47,31	28,48	14,79	48,57
Al	280,02	355,55	357,62	460,10	190,25	356,38	387,96	1113,20	722,04	544,99	614,45	516,50	689,24	354,23	132,78	297,94	641,44	0,71	0,00	0,00	0,72	0,89	0,00	0,00	0,00	1,32	0,00	0,03	
V	21,71	26,94	27,36	37,71	27,23	35,55	35,95	45,56	28,15	46,14	47,10	40,62	25,00	20,86	21,93	6,08	25,82	0,15	0,10	0,08	0,05	0,06	0,03	0,02	0,05	0,01	0,02	0,05	0,08
Si	30,58	28,07	14,89	20,88	21,31	23,81	30,95	23,55	13,79	21,22	23,17	17,47	24,29	12,20	23,16	28,98	25,02	13,85	4,30	2,31	5,65	8,46	9,62	0,00	8,15	9,30	10,87	3,00	11,12
P	16,50	27,10	29,26	33,31	14,99	14,65	14,31	52,04	23,41	56,09	40,18	28,93	14,28	26,25	24,02	4,07	11,22	0,00	3,01	2,05	0,00	0,00	2,45	0,76	1,11	0,00	1,56	6,88	7,81
Li	10,92	14,88	15,07	21,52	14,54	18,62	18,99	23,61	15,08	19,26	22,51	16,66	10,42	10,24	12,84	4,10	11,66	15,81	6,93	8,24	29,13	33,94	23,99	15,18	20,27	3,53	4,02	3,23	4,67
Cu	31,27	24,94	7,53	17,89	15,90	19,80	33,21	50,64	28,91	41,85	30,21	31,27	42,91	19,86	11,51	2,63	51,25	0,88	0,00	0,00	1,05	2,72	0,65	0,00	0,01	4,54	0,00	0,02	0,00
Zn	52,21	68,71	67,28	91,20	60,50	82,24	87,23	140,51	86,32	105,22	105,98	88,93	77,46	57,62	49,60	35,56	79,77	33,77	22,67	21,01	14,07	13,73	14,90	14,19	14,77	6,47	10,94	9,14	4,15
Kr	0,00	0,00	0,00	0,00	0,00	0,00	0,00	0,00	5,82	0,00	17,09	13,01	0,00	19,95	19,58	0,00	20,09	4,39	0,00	17,17	0,00	19,20	0,00	0,00	27,20	0,00	0,00		
Rb	14,74	17,33	16,36	22,00	15,57	21,92	22,42	42,29	26,14	30,13	30,78	27,10	19,45	15,43	13,56	8,33	21,92	0,29	1,64	1,66	6,24	3,85	3,40	20,05	2,54	5,93	6,16	3,32	6,97
Ba	5,84	5,88	3,27	5,05	2,61	2,77	7,55	3,00	3,05	6,77	9,71	7,26	11,94	4,49	3,25	6,33	12,64	35,36	25,23	26,06	26,46	31,44	26,46	17,01	24,50	7,67	0,82	0,61	2,71
Ti	1,73	1,46	1,86	2,41	0,76	1,05	1,37	6,17	4,43	1,93	1,43	1,24	2,13	1,39	0,46	2,87	1,89	0,00	1,46	0,86	0,00	0,00	39,93	0,00	0,00	0,00	0,83	1,71	8,48
Au	3,90	34,93	12,83	7,89	4,56	3,01	2,04	0,00	0,00	0,00	0,00	0,00	0,00	0,00	0,00	0,00	0,00	4,29	0,00	0,00	3,62	2,59	0,00	0,00	0,00	0,00	0,00		
Ni	0,10	10,48	0,20	11,60	0,02	11,14	12,20	0,53	0,34	0,35	0,51	0,39	11,29	10,95	0,00	2,46	0,33	0,84	0,00	0,00	0,18	0,14	0,07	0,00	0,04	0,09	0,00	0,03	0,08
Cr	0,92	1,19	1,14	1,37	0,69	1,12	1,37	3,05	1,98	1,77	1,84	1,62	1,78	1,11	0,69	0,68	1,60	0,00	0,00	0,00	0,00	0,00	0,00	0,00	0,01	0,00	0,02	0,03	0,02
Se	0,00	0,44	0,00	1,30	0,07	0,73	0,11	0,20	1,66	0,02	0,68	0,20	0,41	0,00	0,33	0,21	1,45	0,43	1,97	3,96	3,00	1,66	0,00	0,20	0,26	2,49	0,01		
Co	0,60	0,73	0,77	1,15	0,19	0,90	1,00	1,89	1,22	2,08	2,51	2,13	0,93	0,50	0,06	0,36	1,37	0,00	0,01	0,01	0,06	0,07	0,05	0,02	0,06	0,32	0,02	0,01	0,01
Sn	0,90	0,80	0,31	0,51	0,47	0,44	0,69	0,84	0,48	0,61	0,51	0,46	0,63	0,48	0,37	0,04	0,60	0,00	0,00	0,00	0,00	0,00	0,00	0,00	0,00	0,00	0,00		
Ga	0,34	0,57	0,43	0,61	0,34	0,43	0,55	1,13	0,64	0,61	0,75	0,69	0,21	0,05	0,32	0,24	0,41	0,00	0,02	0,00	0,01	0,02	0,01	0,00	0,03	0,00	0,00		
Pb	0,07	0,21	0,17	0,00	0,46	0,29	0,33	0,01	0,00	0,00	0,33	1,15	0,06	0,31	1,33	0,64	0,00	0,97	0,50	0,51	0,10	0,11	0,00	0,13	0,03	0,00	0,00	0,20	0,20
As	0,20	0,15	0,08	0,15	0,28	0,15	0,07	1,84	0,86	0,83	0,42	0,51	0,49	0,38	0,75	0,04	0,21	0,02	0,05	0,00	0,00	0,06	0,00	0,00	0,00	0,00	0,00		
Cs	0,26	0,31	0,32	0,42	0,28	0,39	0,41	0,82	0,53	0,53	0,56	0,46	0,37	0,27	0,23	0,18	0,40	0,06	0,07	0,08	0,07	0,06	0,06	0,16	0,07	0,02	0,01		0,03
U	0,25	0,34	0,33	0,46	0,34	0,38	0,38	0,65	0,39	0,58	0,57	0,52	0,58	0,37	0,36	0,12	0,41	0,00	0,00	0,00	0,01	0,01	0,07	0,03	0,02	0,00	0,01	0,03	0,04
Ce	0,34	0,42	0,39	0,41	0,10	0,24	0,34	0,77	0,59	0,36	0,30	0,25	0,53	0,45	0,09	0,45	0,69	0,02	0,02	0,02	0,08	0,10	0,05	0,02	0,06	0,04	0,00		
La	0,35	0,45	0,39	0,48	0,12	0,26	0,39	0,75	0,53	0,40	0,37	0,31	0,51	0,47	0,11	0,29	0,63	0,02	0,02	0,01	0,05	0,06	0,05	0,01	0,03	0,03	0,00		
Xe	0,00	0,00	0,00	0,00	0,00	0,00	0,00	0,00	0,00	0,79	0,00	0,00	0,00	0,00	0,00	0,00	0,03	0,00	0,00	0,00	0,00	0,28	0,00	0,00	1,56	1,49	0,00		
Sc	0,04	0,16	0,20	0,22	0,04	0,13	0,13	0,76	0,47	0,19	0,19	0,11	0,43	0,23	0,13	0,16	0,25	0,00	0,00	0,00	0,03	0,01	0,04	0,01	0,02	0,00	0,01		
Th	0,01	0,56	0,23	0,17	0,07	0,08	0,06	0,11	0,10	0,20	0,00	0,01	0,58	0,16	0,00	0,00	0,26	0,01	0,00	0,00	0,01	0,01	0,17	0,00	0,00	0,00	0,00	0,03	0,04
Mo	0,11	0,03	0,01	0,03	0,00	0,00	0,00	0,37	0,28	0,32	0,28	0,28	0,15	0,07	0,03	0,00	0,14	0,00	0,00	0,00	0,00	0,00	0,01	0,00	0,00	0,00	0,04	0,06	0,13
Sb	0,18	0,12	0,02	0,07	0,06	0,07	0,09	0,36	0,21	0,08	0,06	0,09	0,21	0,11	0,08	0,04	0,28	0,00	0,00	0,00	0,00	0,00	0,01	0,00	0,01	0,00	0,00		
Tl	0,06	0,08	0,09	0,11	0,07	0,10	0,10	0,17	0,11	0,10	0,12	0,09	0,10	0,06	0,04	0,05	0,10	0,06	0,00	0,00	0,08	0,08	0,00	0,00	0,00	0,06	0,03		
Be	0,07	0,06	0,07	0,11	0,10	0,06	0,09	0,09	0,13	0,10	0,07	0,04	0,13	0,02	0,02	0,04	0,12	0,00	0,00	0,00	0,00	0,00	0,00	0,00	0,00	0,00	0,00		

Solid samples

Crystalline phases	Scores			
	7DAL5	**7DAL7-S**	**7YL-S3**	**7YL-w2cryst**
NaCl	44	63	35	
$CaPO_3$ (OH). $2H_2O$	8			
NaAl (CO_3) (OH)$_2$	0			
CaPO3 (OH) 2H2O		41		
$KMgCl_3 6H_2O$			60	54
FeS			23	
$MgFe_2O_4$			20	
$Na(NO_3)$			13	
TiO_2			34	
Fe_2Si				25
Ca_2Mg Cr_2 (SiO_4)				18
FeSe				21

Table S3. Chaotropicity, ionic strength and water activity for a selection of samples of the Dallol area.
Chaotropicity and ionic strength values were calculated using Na, K, Mg, Ca, Fe chemistry data; water activity values were measured using a probe (see Methods). Known limits for life for each parameter are listed at the top of the table. Samples beyond that threshold for one or more of those parameters are shaded in grey.

		Chaotropicity (kJ/kg)	Ionic strength (mol/L)	Water activity (a_w)
Life threshold*		**≤87.3**	**≤12.141**	**≥0.585**
Cave water	Gt	n.d	n.d	0,728
	7Gt	-23,797	4,751	0,729
	8Gt	-56,649	6,873	0,731
Lake Assale	8Kar	7,103	7,274	0,718
Geothermally influenced Salt Plain	PS3	24,091	7,138	n.d
Dallol dome hydrothermal pools	DAL 4.00	-17,874	6,104	0,719
	DAL 4.0	-18,712	7,307	n.d
	DAL 4A	-9,607	6,346	n.d
	DAL 4D	2,137	7,104	n.d
	DAL 6A	-23,966	7,203	n.d
	DAL 9A	-7,774	7,529	n.d
	DAL 9C	-16,148	8,349	n.d
	7DAL4-W1	40,435	6,314	0,667
	7DAL4-W2	14,285	5,383	0,698
	7DAL7	19,642	5,989	0,694
	7DAL-N1	20,844	6,472	0,694
	7DAL-N2	11,013	5,940	0,698
	7DAL9	2,948	5,176	0,708
	7DAL10	-7,456	5,037	0,714
	7DAL10-1	n.d	n.d	**0,580**
	7DAL12	-20,574	5,793	n.d
	7DAL13-W1	-20,132	4,785	0,723
	7DAL14	7,544	5,307	0,748
Black Lake area pools	PSBL1	n.d	n.d	**0,334**
	PSBL2	n.d	n.d	**0,345**
	PSBL3	n.d	n.d	0,722
	PSBL4	n.d	n.d	0,711
Black Lake	BL	**354,194**	**19,155**	**0,319**
	7BL-W1	**259,407**	**14,206**	**0,322**
	7BL-W2	**268,893**	**14,721**	n.d
Yellow Lake	YL1	**492,064**	**19,141**	n.d
	YL2	**574,045**	**22,085**	n.d
	YL3	n.d	n.d	**0,319**
	7YL-W1	**495,013**	**18,446**	**0,261**
	7YL-W2	**328,920**	**13,796**	**0,467**
	7YL-W3	**466,640**	**17,609**	n.d

* Data from Hallsworth et al (2007) and Stevenson et al (2015 and 2017)

Table S4. Sequence data and diversity measurements. *Contaminant sequences included sequences identified in negative controls and/or high similarity to human-associated bacteria; s.e., standard error. Eventual mitochondrial and chloropast 16S rRNA gene sequences were also removed at this step.

Sample name	Initial No. of merged reads	No. of high quality reads	No. of retained reads after chimera check	No. of retained reads after removing contaminants*	No. archaeal reads	No. OTUs	Diversity (Simpson index)	Evenness	Richness (Chao1) (s.e.)	No. of bacterial reads	No. OTUs	Diversity (Simpson index)	Evenness	Richness (Chao1) (s.e.)
Prokaryotic sequences							Archaea					Bacteria		
DAL4.0	169949	169648	165257	4	3	2	0,44	0,92	2 (0)	1	1	0,00	NA	1 (0)
DAL4A	152469	152298	146065	5023	5023	2	0,00	0,01	2 (0)	0	0	1,00	0,00	0 (NA)
DAL4C	126853	126665	123020	0	0	0	1,00	0,00	0 (NA)	0	0	1,00	0,00	0 (NA)
DAL4D	125034	124804	120619	0	0	0	1,00	0,00	0 (NA)	0	0	1,00	0,00	0 (NA)
DAL6A	234168	233935	224050	4314	4303	21	0,03	0,03	35 (11)	11	4	0,45	0,64	7 (4)
DAL8-01	113894	112383	108675	6	0	0	1,00	0,00	0 (NA)	6	2	0,28	0,65	2 (0)
DAL8-02	182460	176331	172030	2	0	0	1,00	0,00	0 (NA)	2	2	0,50	1,00	3 (2)
DAL8-03	154815	151700	148869	41	0	0	1,00	0,00	0 (NA)	41	4	0,34	0,49	4 (0)
DAL9A	132758	131862	126420	2	0	0	1,00	0,00	0 (NA)	2	2	0,50	1,00	3 (2)
DAL9C	107108	106589	104746	0	0	0	1,00	0,00	0 (NA)	0	0	1,00	0,00	0 (NA)
7DA7	133151	132970	128002	1	1	1	0,00	NA	1 (0)	0	0	1,00	0,00	0 (NA)
7DA7-pp	42089	42043	41253	2	2	2	0,50	1,00	3 (2)	0	0	1,00	0,00	0 (NA)
7DA9	158516	158249	152576	1821	1	1	0,00	NA	1 (0)	0	0	1,00	0,00	0 (NA)
7DA9-pp	217467	217096	192709	2	0	0	1,00	0,00	0 (NA)	2	1	0,00	NA	1 (0)
7DA10	213263	212784	205528	1	1	1	0,00	NA	1 (0)	0	0	1,00	0,00	0 (NA)
7DA10-pp	44566	44540	40224	62	0	0	1,00	0,00	0 (NA)	62	2	0,03	0,12	2 (0)
7DA14	168809	168500	162187	2096	2094	5	0,01	0,02	5 (0)	2	2	0,50	1,00	3 (2)
7DA14-pp	82248	82170	71068	471	345	30	0,94	0,89	32 (3)	126	7	0,69	0,72	7 (0)
7DA2-01	33880	33832	33711	45	31	5	0,68	0,82	5 (0)	14	7	0,83	0,94	9 (3)
7DA4-s	103418	103261	102476	1492	1490	13	0,81	0,69	15 (3)	2	2	0,50	1,00	3 (2)
7DA5-s	184910	184641	180701	5243	3208	22	0,91	0,82	32 (10)	2035	19	0,84	0,78	19 (0)
7DA9-s	130399	130259	129730	261	212	8	0,72	0,70	9 (1)	49	1	0,00	NA	1 (0)
7DA13-s	100425	100280	99550	298	298	7	0,66	0,67	7 (0)	0	0	1,00	0,00	0 (NA)
7DA15-s	143741	143552	142694	12589	12460	11	0,06	0,08	11 (0)	129	2	0,48	0,97	2 (0)
YL1	226774	226389	217444	42	1	1	0,00	NA	1 (0)	41	4	0,30	0,43	5 (2)
7YL	178284	177903	172455	1770	1302	13	0,57	0,47	13 (0)	468	7	0,74	0,76	7 (0)
7YL-pp	65597	65556	62547	0	0	0	1,00	0,00	0 (NA)	0	0	1,00	0,00	0 (NA)
YL2	153107	152918	144028	2	2	1	0,00	NA	1 (0)	0	0	1,00	0,00	0 (NA)
YL3-01w	188511	188312	172260	126	0	0	1,00	0,00	0 (NA)	126	3	0,03	0,08	4 (2)
YL3-01s	232822	232611	210691	3	0	0	1,00	0,00	0 (NA)	3	2	0,44	0,92	2 (0)
7YL-s3	158645	158488	157145	979	898	15	0,86	0,83	15 (0)	81	4	0,07	0,14	7 (4)
7YL-s4	86468	86366	85180	207	157	4	0,60	0,76	4 (0)	50	2	0,08	0,24	2 (0)
YL4.01	200889	200588	191536	10711	10691	2	0,00	0,00	2 (0)	20	3	0,27	0,47	3 (0)
7YL-s1	124032	123877	122505	36177	36016	39	0,79	0,50	39 (0)	161	6	0,79	0,91	6 (0)
7YL-s2	85188	85072	84444	668	547	10	0,75	0,70	10 (0)	121	5	0,71	0,83	5 (0)
BL2	76395	76209	73977	12	0	0	1,00	0,00	0 (NA)	12	6	0,78	0,91	8 (3)
BLw	227966	227636	218708	0	0	0	1,00	0,00	0 (NA)	0	0	1,00	0,00	0 (NA)
7BLw1	177297	177131	171404	3	0	0	1,00	0,00	0 (NA)	3	1	0,00	NA	1 (0)
7Blw2	158986	158630	151304	1	0	0	1,00	0,00	0 (NA)	1	1	0,00	NA	1 (0)
PSBL1	127518	127100	124137	8	0	0	1,00	0,00	0 (NA)	8	4	0,66	0,88	5 (1)
PSBL2	181312	180562	177286	5	3	2	0,44	0,92	2 (0)	2	1	0,00	NA	1 (0)
PS3	150482	149968	146028	146028	118980	291	0,88	0,56	313 (7)	26537	123	0,96	0,56	138 (11)
PS	304190	303656	282495	282495	274013	602	0,94	0,51	701 (22)	5893	39	0,30	0,51	50 (8)
ASS	173226	172959	165299	165299	140633	1013	0,94	0,59	1190 (33)	23963	496	0,69	0,59	544 (13)
ASS-PJ	314682	314213	288299	288299	244551	1349	0,94	0,57	1441 (18)	39873	859	0,88	0,57	912 (12)
GT	303592	303083	288086	288086	274039	656	0,87	0,53	755 (25)	14047	173	0,91	0,53	193 (11)
7GT	71483	71368	64143	64143	59788	524	0,95	0,57	735 (46)	4353	147	0,92	0,57	201 (22)
7Gt-pp	235497	235111	172010	172010	132967	1495	0,97	0,57	1565 (13)	39039	227	0,77	0,57	253 (10)
GC	198582	198288	189428	32807	30700	68	0,71	0,40	80 (7)	2107	2	0,00	0,01	2 (0)
GC2	94053	93926	87922	16162	15575	64	0,83	0,50	71 (5)	587	1	0,00	NA	1 (0)
7CMcore	135254	135086	133629	202	136	16	0,55	0,50	19 (3)	66	1	0,00	NA	1 (0)
7Gt2	150640	150409	138429	14250	7334	33	0,64	0,43	36 (4)	6916	18	0,64	0,48	19 (1)
NEGATIVE CONTROL A	106471	105571	96569	94348	2876	19	0,69	0,49	26 (7)	91472	351	0,97	0,69	461 (36)
NEGATIVE CONTROL B	149421	148866	140175	135739	2782	16	0,83	0,72	17 (2)	132957	484	0,97	0,72	555 (20)
Eukaryotic sequences														
8Ass	320243	319549	312333	307451		306	0,68	0,25	308 (2)					
Ass	148963	148396	142049	140678		122	0,65	0,31	136 (7)					
PS	83526	83207	82325	82316		50	0,06	0,04	55 (4)					
PS3	87971	87459	86745	54		6	0,36	0,46	6 (0)					
Gt	15063	14998	14883	1795		4	0,25	0,34	4 (0)					
8Gt	57995	57773	56359	56269		125	0,56	0,23	125 (0)					

Table S5. Mineral phases observed by SEM-EDX in precipitates of typical abiotic morphology and 'biomorphs'. Biomorphs correspond to rounded-shaped crystalline morphs resembling cell structures (cocci, rods) and compatible with cellular sizes. Observed dominant phases are highlighted in bold

Site	Samples	Mineral phases	
		Typical 'crystals'	Abiotic 'Biomorphs'
Cave water	Gt2016, 7Gt, 8Gt_1	Si, Ca sulfate, Fe-K sulfate, Al-Mg-Fe oxides, Fe and Ca oxides	Fe-Al silicates
Lake Assale (Karum)	8Ass_2, 8Ass_3, 8Ass_4, 8Ass_6, 8Ass_7, 8Ass_8	NaCl, Na-K-Mg chloride	**Si biomorphs** (and encrustment)
Dallol dome (ponds)	Dal4.0, 7DA7_07, DAL4D, 7DA9-P1, 7CA9_P1_3, 7DA7_04, 7DA7_05, 7DA7_06, 7DA9_P1_2, 7DA9_P1_5, 7DA9_P3_10, 7DA9_P3_12	NaCl, Na-K-Mg chloride, Fe-K oxides(?), Ti oxides	Sulfur biomorphs, **Si biomorphs**, S-rich Na-K silicates, locally S-rich Si biomorphs, **Fe phosphates**, Fe-K phosphate, Si biomorphs – enriched in Fe, Mg, K and locally S
Yellow lake	YL1-03_4, 7YL_4, YL1-03_5, 7YL_6	Fe chloride, Mg chloride	Si, $CaCl_2$, Ca phosphate
Black lake area (ponds)	BLPS_05_5	Mg-Fe-K chloride	Mg chloride

Other Supplementary Materials for this manuscript include the following:

Data S1. (Table) Organic and ionic chromatography analysis of samples from the Dallol dome and surrounding area.

Data S2. (Table) Identification, phylogenetic affinity and relative abundance of prokaryotic OTUs.

Data S3. Identification, phylogenetic affinity and relative abundance of eukaryotic OTUs from Dallol area samples.

Data S4. Full tree of archaeal 16S rRNA gene fragments in Newick format.

Data S5. Full tree of bacterial 16S rRNA gene fragments in Newick format.

Data S6. Chemical maps obtained from energy dispersive X-ray spectrometry (EDXS) combined to SEM observations of cells and abiotic biomorphs observed in the Dallol area and Lake Assale (Karum).

Data S7. Energy dispersive X-ray spectrometry (EDXS) spectra of different structures observed in samples from the Dallol area.